Journal of
Ship&Ocean
Technology
©MARCH 2008

SOTECH Vol. 12, No. 1, pp. 16 ~ 27, 2008

Numerical Simulation of Wave Breaking Near Ship Bow

Young-Gill Lee[1], Nam Chul Kim[2], Jin-Won Yu[3] and Si-Young Choi[3]

[1] Department of Naval Architecture and Ocean Engineering, Inha University, Incheon, Korea
[2] Regional Research Center for Transportation System of Yellow Sea, Inha University, Incheon, Korea
[3] Department of Naval Architecture, Graduate School of Inha University, Incheon, Korea; Corresponding Author: younglee@inha.ac.kr

Abstract

The interaction between advancing ships and the waves generated by them plays important roles in wave resistances and ship motions. Wave breaking phenomena near the ship bow at different speeds are investigated both numerically and experimentally. Numerical simulations of free surface profiles near the fore bodies of ships are performed and visualized to grasp the general trend or the mechanism of wave breaking phenomena from moderate waves rather than concentrating on local chaotic irregularities as ship speeds increase. Navier-Stokes equations are differentiated based on the finite difference method. The Marker and Cell (MAC) Method and Marker-Density Method are employed, and they are compared for the description of free surface conditions associated with the governing equations. Extra effort has been directed toward the realization of extremely complex free surface conditions at wave breaking. For this purpose, the air-water interface is treated with marker density, which is used for two layer flows of fluids with different properties. Adaptation schemes and refinement of the numerical grid system are also used at local complex flows to improve the accuracy of the solutions. In addition to numerical simulations, various model tests are performed in a ship model towing tank. The results are compared with numerical calculations for verification and for realizing better, more efficient research performance. It is expected that the present research results regarding wave breaking and the geometry of the fore body of ship will facilitate better hull form design productivity at the preliminary ship design stage, especially in the case of small and fast ship design. Also, the obtained knowledge on the impact due to the interaction of breaking waves and an advancing hull surface is expected to be applicable to investigation of the ship bow slamming problem as a specific application.

Keywords: free surface, breaking wave, finite difference method, two-phase flow, marker-density method

1 Introduction

Resistance acting on a ship hull due to waves generated by an advancing ship tends to increase as the ship speed increases. As an extreme case, the wave resistance of a high

speed ship reaches almost half the whole resistance against the advancing ship. Among phenomena involved in the wave resistance problem, wave breaking becomes more apparent and critical as the speed increases, thus necessitating special attention from naval architects and hydrodynamic experts. The interaction between an advancing ship and breaking waves generated by the ship is an extremely complicated subject among many difficult problems related with free surfaces. The MAC (Marker and Cell) method was introduced by Welch in 1966 to investigate an incompressible fluid flow problem having a free surface. The MAC technique uses particles with no mass nor volume distributed in the whole free surface of a fluid to trace the free surface. The massless particles are fictitious, of Lagrangian type, and play no role in the dynamics of the fluid motion. The instantaneous free surface is determined by the markers with flow advection. In 1970, Chan & Street applied the MAC method to a water wave problem by improving the dynamic boundary conditions at the free surface.

The VOF (Volume Of Fluid) method is another volume tracking type technique, introduced by Hirt & Nichols in 1981. The VOF method is considered to be more efficient than the MAC method in determining more complex interfaces where fluids with different densities meet, as well as where breaking splash and fluid detachment occur, because of its effective numerical scheme, which requires less memory and CPU cost. Several different approaches based on geometrical modifications have been developed out of the original VOF method, including the donor-acceptor algorithm by Ramshaw in 1976 and Fekken in 1999, the SLIC (Simple Line Interface Calculation) algorithm by Noh & Woodward in 1976, the FCT (Flux-Corrected Transport) algorithm by Zalesak in 1979, and the HRIC (High-Resolution Interface-Capturing) technique by Muzaferija in 1999. Azcueta et al. used the HRIC scheme to compute the flow around hydrofoils beneath a free surface and the breaking of bow waves around a ship in motion in 1999. Miyata & Kawamura, in 1994, developed the density function method, which is a product of the density and VOF function, and determined the free surface profile where the value of the density function distributes an intermediate number between 0.0 and 1.0 after both the liquid and gas flows are computed to decide the interfacial free surface using the kinematic and dynamic boundary conditions. This Marker-Density technique, integrating the strengths of the MAC and VOF methods, was used by Miyata in investigating breaking waves at a free surface as an alternative to the MAC method to overcome complex mechanisms involved in free surface phenomena. The LS (Level Set) method was first introduced by Osher & Sethian in 1988 as an Eulerian inter face tracking methods, in which the interfaces are tracked because the zero level set is found explicitly as a part of numerical computations. Surface tension can be easily included in this scheme as well as the momentum and continuity equations.

Breaking waves usually occur in a specific coastal region, the so called surf zone where sea and land meet. In naval architecture, breaking waves are frequently found as a result of interactions between bow waves and ship hulls when ships advance at high speeds. Bow waves are waves that are generated near bows by ships in advance, and their patterns vary with ship speeds. The wave breaking phenomenon itself has also been a subject of great concern among hydrodynamic experts and physical oceanographers, and has been investigated through various approaches, because the phenomenon is extremely complex with velocities that are almost chaotic and vary drastically in time. Vanden Broeck & Tuck, in 1977, investigated wave breakings around the bow generated by an advancing ship with shallow draft, and simulated them in three dimensions. In 1985Mori, investigated similar wave breakings generated by a ship on an irregular wavy free surface. In this research, the

breaking of bow waves is investigated using numerical computations and simulation techniques.

The purpose of the present research is to estimate and compare different methods and choose the most suitable scheme among them with respect to investigating a free surface and related phenomena. The generation of wave breaking is also studied, and we attempt to predict the occurrence of this phenomenon near a ship bow at different ship speeds. Numerical computations were performed via two different methods, the MAC method and Marker-density method. Experiments were also carried out in the ship model basin at Inha University to confirm and compensate for the numerical approaches. Simulations were performed numerically to comprehend overall patterns of wave breaking by comparing the results obtained from the aforementioned two methods. The respective strengths and weaknesses of both methods are also discussed. The two ship models used in the experiments have wedge-shaped bows, transom sterns, and simple aft bodies with a rectangular transverse section. The present research focuses on the free surface regions around ship bows, where most significant wave generation and breaking occur. Mesh adaptation, or the refinement of a grid system, is employed where the local gradients of the variation of physical values are large in order to improve the solution accuracy and to save computer CPU capability.

2 Numerical simulation

2.1 Marker-density method

2.1.1 Governing equations and associated free surface boundary conditions

Assuming that the fluid consists of layers and that it is incompressible, at least in the neighborhood of the interfacial free surface, the governing equations of viscous flow become the Navier-Stokes equations based on Newton's law of motion and a continuity equation obtained from the law of mass conservation as given below:

$$\frac{\partial \vec{u}}{\partial t} = -\frac{\nabla p}{\rho_i} - (\vec{u} \circ \nabla)\vec{u} + \nu_i \nabla^2 \vec{u} + \vec{f} \tag{1}$$

$$\nabla \circ \vec{u} = 0 \tag{2}$$

where i = 1 or 2 are the subscripts for the two fluid layers (1 for the air above and 2 for the water below the interface), $\vec{u} = (u, v, w)$ is the velocity, t the time, ∇ the gradient operator, ρ_i the densities, p the fluid pressure, ν_i the kinematic viscosities, and $\vec{f}$ all external forces. Nonlinear free surface boundary conditions are used to determine the free surface configuration without any simplification. Those nonlinear dynamic and kinematic boundary conditions are:

$$p_1 = p_2 \tag{3}$$

$$\frac{D(M_\rho)}{Dt} = 0 \tag{4}$$

where D is a substantial derivative operator and M_ρ is the density function. Equation (3) is the dynamic condition requiring that there be no pressure jump at the interface between the two fluid layers. Equation (4) is the marker-density function equation replacing the ordinary condition requiring that water particles move with the free surface. Because the usual kinematic boundary requirement is generally insufficient with respect to handling complicated free surfaces such as surging or breaking waves, the marker-density function equation (4) was developed to overcome problems associated with the marker-density function. The density function takes values between ρ_1 and ρ_2 in the domain during computation, and this represents the porosity in each cell, in other words, the volume fraction of water in a cell. The location of the free surface is determined to be the point where the marker-density function takes the mean value of ρ_1 and ρ_2 at any instant or each time step. The free surface profile obtained using the mean value coincides with the surface elevation that can be determined using the usual kinematic boundary condition. Thus, equation (4) can be a generalized condition of its original.

Model 1 (9.5 deg.)

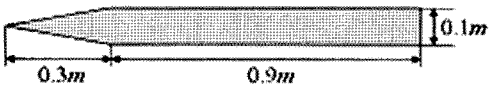

Description	Model (9.5deg.)
Length	1.20 m
Beam	0.10 m
Depth	0.15 m
Draft	0.08 m

Model 2 (18.4 deg.)

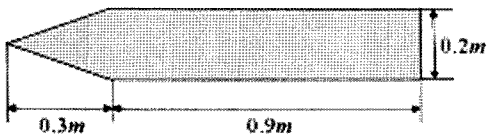

Description	Model (18.4deg.)
Length	1.20 m
Beam	0.20 m
Depth	0.15 m
Draft	0.08 m

Figure 1: Models and their dimensions

The marker-density value is calculated from equation (4) at each time step, and the velocity distribution is updated using the Navier-Stokes equations (1) as time passes. For the discretization of convective terms, a flux-split method with a variable mesh size is employed. For the diffusive terms, a second order centered difference scheme is used while a second order Adam-Bashforth scheme is used for the time integration. The pressure distribution at each time step is calculated through iteration following the usual method using the Poisson equation of pressure. Pressures and velocities at the interface are determined approximately using extrapolation. Pressures are extrapolated with zero gradient in the normal direction to the free surface including the effect of the static pressure difference in that direction due to gravity. Velocities between the two fluid layers are also extrapolated via a similar technique.

Body boundary conditions are comparatively simple to handle as compared with free surface boundary conditions. That is, the usual condition that fluid particles attach to the ship hull and move together at the instant of contact is employed for the numerical computation.

2.1.2 Numerical simulation results

In figure 1, the shapes of the models and their dimensions are displayed. The geometries of the models are intentionally designed simply so as to remove unnecessary factors other than

the bow wave breaking phenomenon itself. Computational conditions for the marker-density method, i.e., cell sizes, time steps, computational domains, etc., are displayed in table 1. Cell sizes are smaller near the ship hull and become larger as the distance increases in accordance with the flow characteristics. Several cases are computed numerically at different ship model speeds from 0.5 m/sec to 1.0 m/sec to verify the effect of speed on wave patterns and breaking behaviors including how waves are initiated and broken and how they are developed to propagate.

Table 1: Computational conditions for marker-density method

Number of cells	X	110
	Y	65
	Z	65
Computational domain	X	0.75 m
	Y	0.55 m
	Z	0.32 m
Cell size	X_{min}	0.006 m
	Y_{min}	0.0045 m
	Z_{min}	0.004 m
Number of time steps		2800

In figure 2, horizontal and vertical cross-sections of the domains with meshes are displayed where the Marker-density method was employed for the simulations or numerical computations

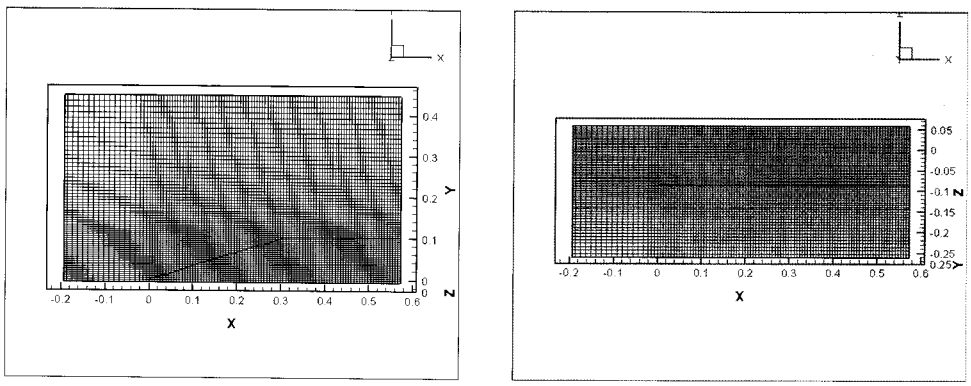

(a) X-Y plan (b) X-Z plan

Figure 2: The domain of simulation for marker-density method

In figure 3, numerically simulated bow waves are displayed in the case of model 1, which has a narrow fore-body

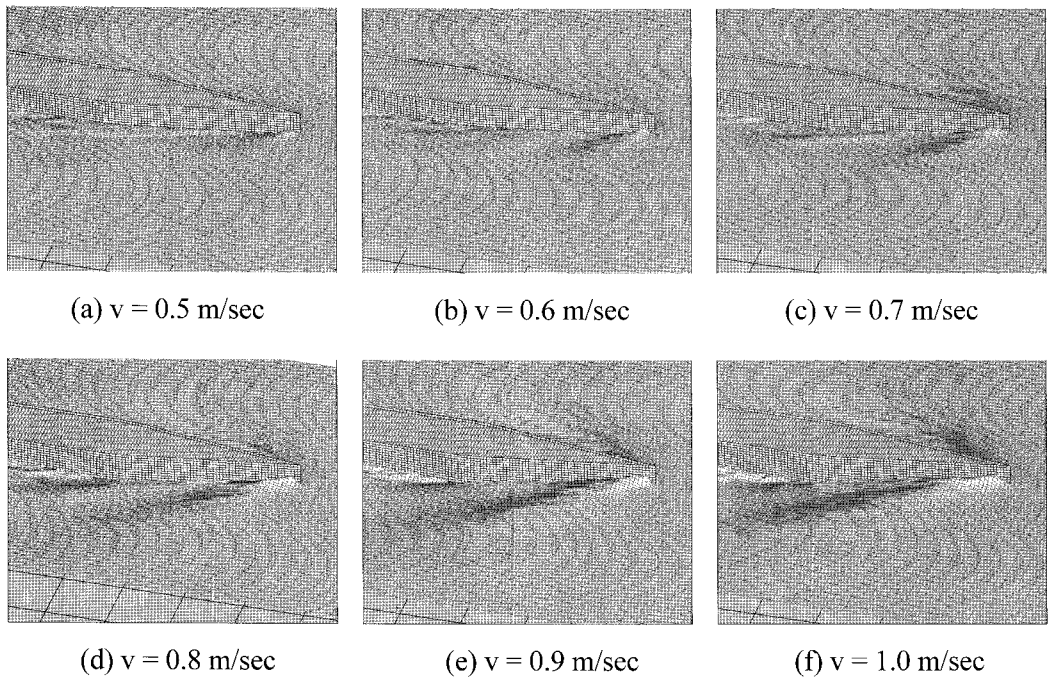

(a) v = 0.5 m/sec (b) v = 0.6 m/sec (c) v = 0.7 m/sec

(d) v = 0.8 m/sec (e) v = 0.9 m/sec (f) v = 1.0 m/sec

Figure 3: Simulations of bow wave breaking at different advancing speeds in the case of model 1

It is apparent that the wave breaking becomes severe and bow waves are developed in scale as the ship speed increases. Around v = 0.6 m/sec, bow waves appear to start breaking under the present numerical set-up. The present simulation shows that there appears another or secondary wave at the shoulder area, being generated by the increase of ship speed. This secondary wave also grows, eventually leading to a breaking phenomenon with increasing ship speed, as seen in the cases of e) and f). It appears that, similar to the bow area, the geometry of the shoulder area causes drastic changes in the free surface flows, sufficient for wave breaking. If the model has a smooth and soft shoulder geometry with good fairing, shoulder wave breaking may not occur or be apparent, as is the case of a well designed yacht. In figure 4, similar bow wave breaking is simulated with model 2, which has an almost twice greater bow angle than model 1. Bow wave breaking occurs more seriously than for model 1, owing to the blunt ship bow geometry, in accordance with ordinary engineering experience and prediction. The case of f) shows more severe wave breaking in a wider region, which means that more drastic changes are caused in the free surface and underwater flows, which are disrupted by the advancing blunt bow. However, the shoulder wave breaking in this case is less apparent than the previous case at similar ship speeds, it is conjectured that the phenomena are caused by the larger entrance angle or blunt fore-body shape may prevent the free surface flow from reaching sufficient velocity to generate collapsing or breaking waves around the shoulder area

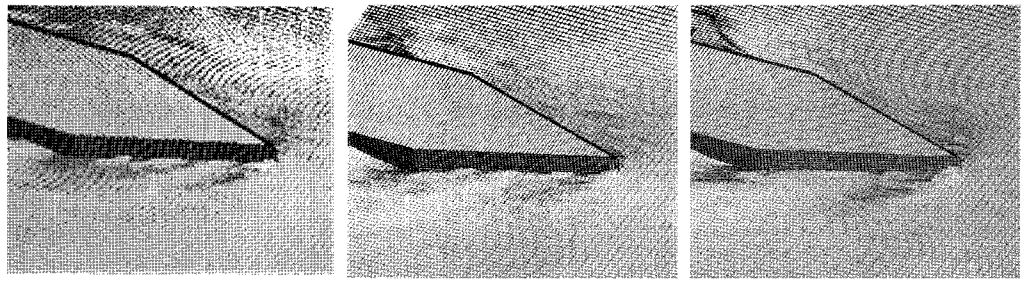

(a) v = 0.5 m/sec (b) v = 0.6 m/sec (c) v = 0.7 m/sec

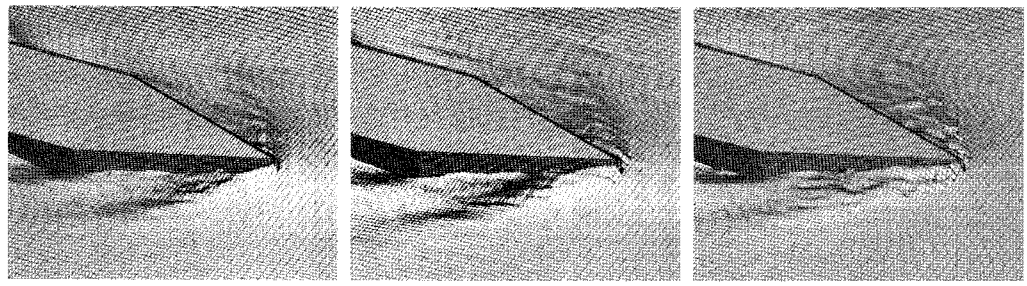

(d) v = 0.8 m/sec (e) v = 0.9 m/sec (f) v = 1.0 m/sec

Figure 4: Simulations of bow wave breaking at different advancing speeds in the case of model 2

2.2 Marker and cell method

2.2.1 Governing equations and associated free surface boundary conditions

Assuming that the water is an incompressible and inviscid fluid, the usual Euler type momentum equations and the continuity equation can be used to describe or investigate the bow wave breakings. For the numerical simulation, the governing equations associated with both free surface and body boundary conditions are differentiated: the convective terms are differentiated using a hybrid scheme of second order centered finite difference and a donor cell method, and the remaining terms are of first order forward finite difference with respect to time and of second order centered finite difference with respect to space. The free-slip requirement is employed for the body boundary conditions. Free surface boundary conditions are as follows, without the effects of viscosity and surface tension:

$$p = p_a \tag{5}$$

$$\frac{D(\varsigma - z)}{Dt} = u\frac{\partial(\varsigma - z)}{\partial x} + v\frac{\partial(\varsigma - z)}{\partial y} + w\frac{\partial(\varsigma - z)}{\partial z} + \frac{\partial(\varsigma - z)}{\partial t} = 0 \tag{6}$$

where p_a is the atmospheric pressure and ς is the surface elevation. Equation (5) is the dynamic boundary condition requiring that the water pressure match the air pressure at the interface, and equation (6) is the kinematic boundary condition stating that water particles attach to the free surface and move with it. In this method, markers with no mass or volume are distributed throughout the fluid surface (water surface in this case) to trace the gravitational free surface. The fictitious Lagrangian type particles play no role in the dynamics of fluid motion. The instantaneous free surface is determined by the markers with flow advection using numerical iteration at each time step

2.2.2 Numerical simulation results

In table 2, computational conditions for the MAC method are displayed, such as the number of cells, the domain of computations, etc.. In figure 5, numerical simulations of model 1 are displayed at three different speeds. Although we have computed more cases at other speeds, they are not shown here because the simulated results by MAC methods.

Table 1: Computational conditions for MAC method

Number of cells	X	85
	Y	60
	Z	40
Computational domain	X	0.75 m
	Y	0.52 m
	Z	0.20 m
Cell size	X_{min}	0.006 m
	Y_{min}	0.004 m
	Z_{min}	0.005 m
Number of time steps		1500

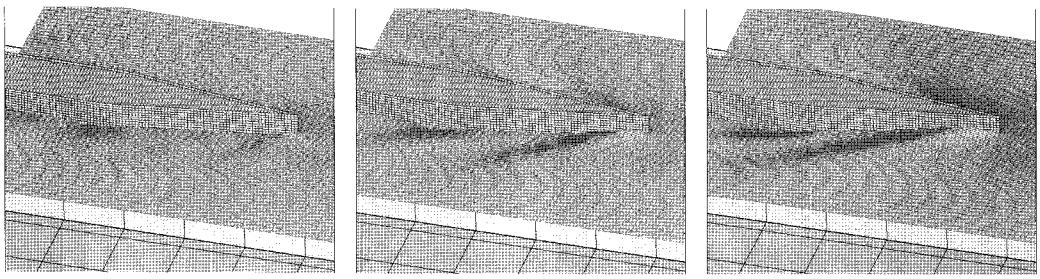

(a) v = 0.5 m/sec (b) v = 0.8 m/sec (c) v = 1.0 m/sec

Figure 4: Simulations of bow wave patterns at different advancing speeds in the case of model 1

3 Experiment in towing tank

The bow wave breaking phenomenon is also simulated experimentally in the towing tank of Inha University using models 1 and 2 with the same dimensions as indicated in figure 1. Data and experimental parameters were chosen to be the same as those of numerical simulations so that the results could be compared with those from the experimental approach.

In Figures 6 and 7, different simulation results are summarized and compared graphically when the breaking is fully developed at each approach during the research. On the whole, the simulations by the Marker-density method are more realistic or closer to the results obtained by experiments, thus implying that this method is superior to the MAC method. This trend is more apparent in figure 7. Graph (c) obtained by the Marker-density method shows good resemblance to photo (b) taken during the experiments.

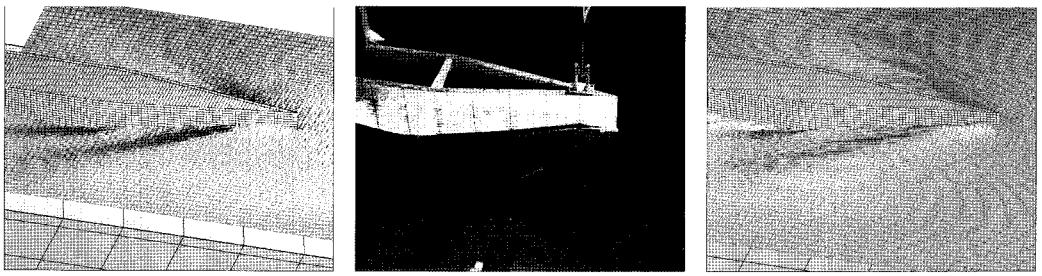

(a) v =1.0 m/sec, MAC (b) v = 1.0 m/sec, experiment (c) v = 1.0 m/sec, Marker-density

Figure 6: Comparison of different simulations of bow wave breakings in the case of model 1

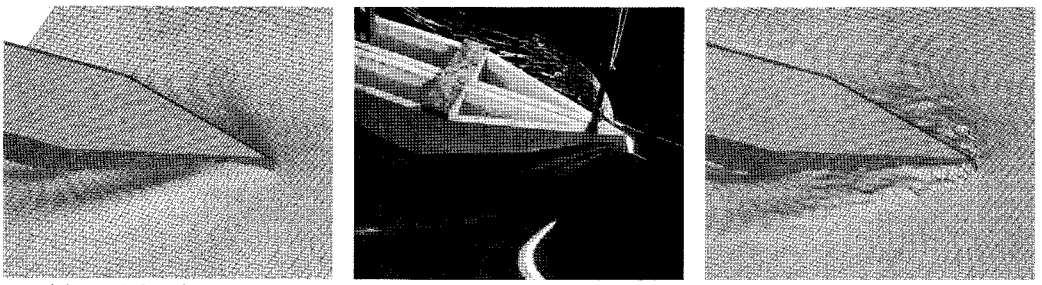

(a) v =1.0 m/sec, MAC (b) v = 1.0 m/sec, experiment (c) v = 1.0 m/sec, Marker-density

Figure 7: Comparison of different simulations of bow wave breakings in the case of model 2

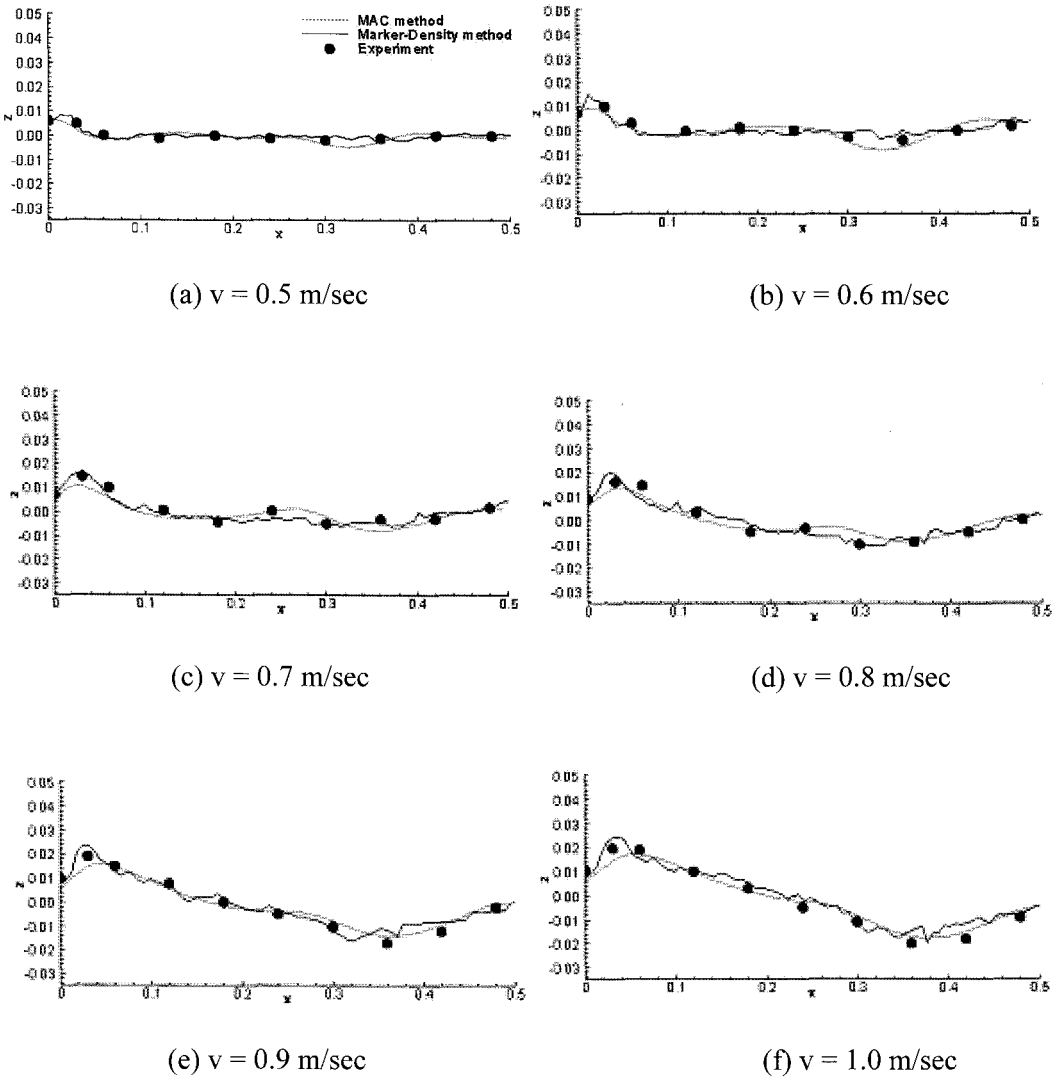

(a) v = 0.5 m/sec (b) v = 0.6 m/sec

(c) v = 0.7 m/sec (d) v = 0.8 m/sec

(e) v = 0.9 m/sec (f) v = 1.0 m/sec

Figure 8: Comparison of wave profiles along the hull surface in the case of model 1

Wave profiles along the hull surface from the towing model test and numerical simulation are compared in Figures 8 and 9 to validate the numerical simulation results. Figure 8 shows the numerical results performed in the case of model 1, and Figure 9 shows those performed in the case of model 2. The numerical results using the MAC and Marker-density methods and experimental results show good agreement with each other. However, observing the region near the bow, the results obtained using the Marker-density method are relatively good agreement with the experimental results than those gathered using the MAC method. It is shown near the bow expected wave breaking.

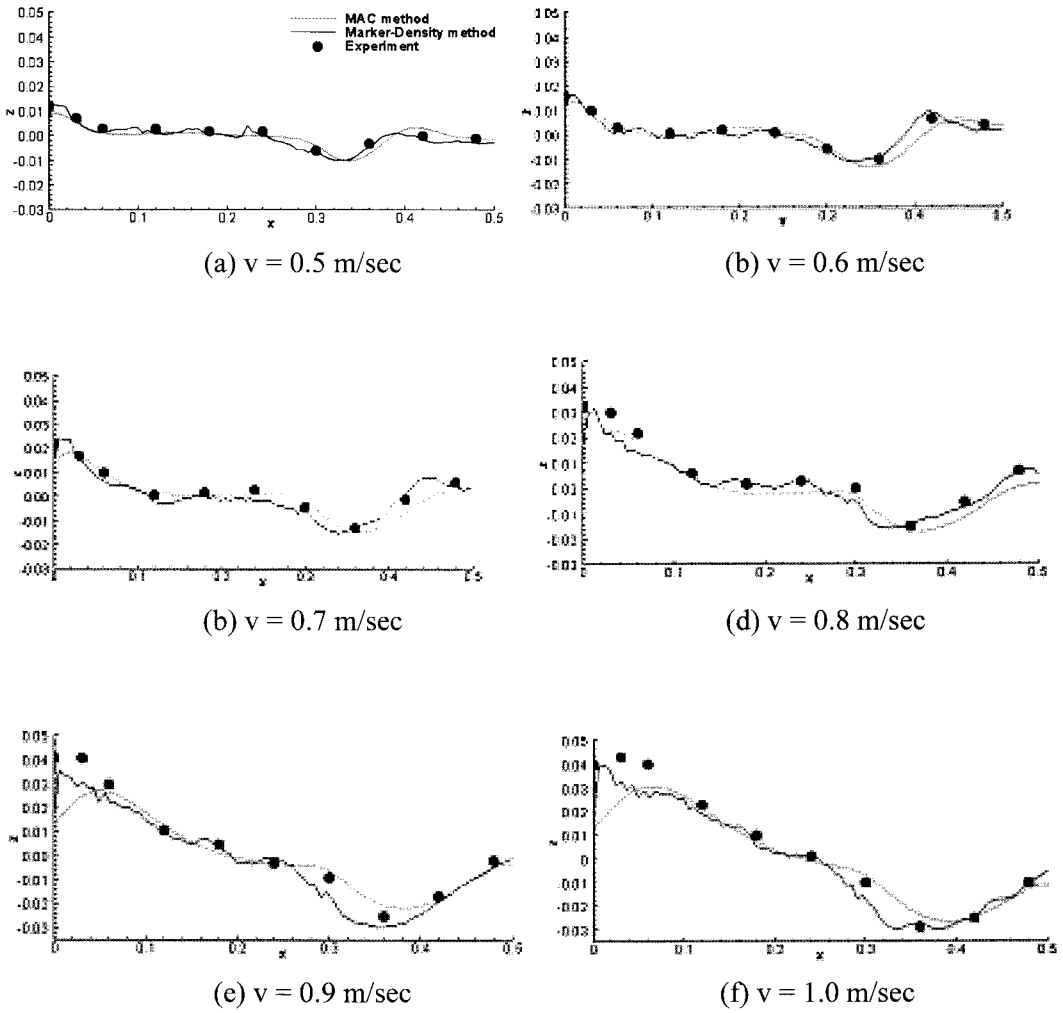

(a) v = 0.5 m/sec (b) v = 0.6 m/sec

(b) v = 0.7 m/sec (d) v = 0.8 m/sec

(e) v = 0.9 m/sec (f) v = 1.0 m/sec

Figure 9: Comparison of wave profiles along the hull surface in the case of model 2

6 Conclusion

The bow wave breaking phenomenon is investigated and interpreted by way of numerical and experimental simulations. The numerical simulations are performed using the Marker-density method and Marker and Cell Method. The experimental simulations are carried out in the ship model towing tank at Inha University. Both numerical and experimental simulations are performed using the same data and parameters, as much as possible, such as ship speed, cell size, mesh type, etc.. Simulations by the Marker-density method show good resemblance with experimental simulations. On this ground it is concluded that the Marker-density method is superior to the old MAC method in

investigating bow wave breaking and similar complicated problems regarding free surface phenomena.

Acknowledgements

This paper is based on the intermediate results of an ongoing project supported by the Basic Research Program of KOSEF (Korea Science & Engineering Foundation), Grant No. - R01-2005-000-10878-0.

Reference

Azcueta, R., S. Muzaferija and M. Peric. 1999. Computation of Breaking Bow Waves for a Very Full Hull Ship. Proc. 7th Int. Conf. on Numerical Ship Hydrodynamics, Nantes, France.

Chan, R.K. and R.L. Street. 1970. SUMMAC-A Numerical Model for Water Wave. Technical Report No.135. Dept. of Civil Engineering: Stanford University, Stanford, USA.

Fekken, G., A.E.P. Veldman and B. Buchner. 1999. Simulation of Green Water Loading Using the Navier-Stokes Equations. Proc. 7th Int. Conf. od Numerical Ship Hydrodynamics, Nantes, France.

Hirt, C.W. and B.D. Nichols. 1981. Volume of Fluid (VOF) Method for The Dynamics of Free Boundaries. Journal of Computational Physics, **39**, 201-205.

Kawamura, T. and H. Miyata. 1994. Simulation of Nonlinear Ship Flows by Density-Function Method. J. Soc. Naval Arch. Japan, **176,** 1-10.

Mori, K.N. 1985. Vortex and bow wave around blunt bodies. Proc. 13th Symp. Naval Hydrodynamics, Germany.

Muzaferia, S. and M. Peric. 1999. Computation of free surface flows using interface-tracking and interface-capturing methods. Chap.2 in O. Mahrenholtz a & Markiewicz, M. (ed.), Nonlinear Water Wave Interaction, 59-100. WIT Press.

Noh, W.F. and P. Woodward. 1976. SLIC(Simple Line Interface Calculation). Proc. 5th Int. Conf. on Numerical Methods in Fluids.

Osher, S. and J.A. Sethian. 1988. Fronts Propagating with Curvature-Dependent Speed: Algorithms Based on Hamilton-Jacobi Formulation. Journal of Computational Physics, **79**, 12-49.

Park, J.-C. and H. Miyata. 1994. Numerical Simulation of 2D and 3D Breaking Waves by Finite Difference Method. J. Soc. Naval Arch. Japan, **175**, 11-24.

Ramshaw, J.D. and J.A. Trapp. 1976. ANumerical Technique for Low-Speed Homogeneous Two-Phase Flow with Sharp Interface. Journal of Computational Physics, **21**, 438-453.

Sethian, J.A. 1999. Level Set Methods and Fast Marching Methods. Cambridge University Press, Cambridge, USA.

Vandan Broeck, J.-M. and E.O. Tuck. 1977. Proc. 2nd Int. Conf. Num. Ship Hydrodynamics, Berkeley, USA.

Welch, J.E., F.H. Harlow, J.P. Shannin and B.J. Daly. 1966. The MAC Method. Los Alamos Science Lab. Report LA-3425, Los Alamos, USA..

Zalesak, S. 1979. Fully Multi-Dimensional Flux-Corrected Transport Algorithms for Fluids. Journal of Computational Physics, **11,** 38-69.